
ELSEVIER
BIORESOURCE
TECHNOLOGY
Effect on H2 evolution
Effect on CO evolution
Effect on CO2 evolution
Effect on CH4 evolution
Time on stream (min)
Available online at www.sciencedirect.com
SciVerse ScienceDirect

Bioresource Technology 137 (2013) 63–73

Contents lists available at SciVerse ScienceDirect

Bioresource Technology

journal homepage: www.elsevier.com/locate/biortech

Radiation and optical properties of *Nannochloropsis oculata* grown under different irradiances and spectra

Razmig Kandilian, Euntaek Lee, Laurent Pilon *

Mechanical and Aerospace Engineering Department, Henry Samueli School of Engineering and Applied Science, University of California, Los Angeles, Los Angeles, CA 90095, USA

HIGHLIGHTS

- *Marine microalgae N. oculata* were grown under white or red LEDs with different irradiances.
- Their absorption and scattering cross-sections were measured in the PAR region.
- Cross-sections and retrieved refraction index did not depend on incident spectra and irradiance.
- Absorption cross-section and absorption index decreased under nutrient limited conditions.

GRAPHICAL ABSTRACT

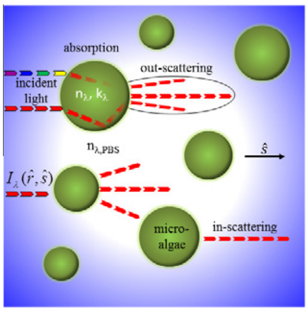

ARTICLE INFO

Article history:
Received 18 November 2012
Received in revised form 6 March 2013
Accepted 9 March 2013
Available online 18 March 2013

Keywords:
Biofuel
Biodiesel
Microalgae
Nannochloropsis oculata
Photobioreactors
Optical properties
Light transfer
Ocean optics

ABSTRACT

This paper reports accurate measurements of the radiation characteristics and optical properties of *Nannochloropsis oculata* in the photosynthetically active radiation (PAR) region. These marine microalgae were grown in 2 cm thick culture bottles with vented caps exposed, on one side, to either white fluorescent light bulbs or red LEDs emitting at 630 nm. The illuminance varied from 2000 to 10,000 lux. The microalgae average equivalent diameter ranged from 2.52 to 2.63 μm. Their radiation characteristics and optical properties were statistically identical over most of the PAR region. Other *N. oculata* grown with 2 vol.% CO_2 injection in 1 cm thick flat bottles exposed to light from both sides reached a significantly larger mass concentration and featured lower pigment concentration and smaller absorption cross-sections. This was due to nutrient limited growth conditions. The refraction index was independent of illuminance, spectrum, and growth conditions and featured resonance at wavelengths corresponding to absorption peaks.

1. Introduction

The vast majority of the energy demand in the world is supplied by fossil fuels which has led to pollution and climate change (Intergovernmental Panel on Climate Change, 2007). Photosynthetic microalgae could be cultivated for producing liquid biofuels in a renewable and sustainable manner (Chisti, 2007). Currently, biofuels are mainly produced from higher plants such as soybean, corn, and sugar cane (Chisti, 2007). Cultivating these plants to produce fuels have proved controversial due to the use of food crops requiring large amounts of freshwater and large surface area of arable land (Chisti, 2007). Microalgae, on the other hand, are single cell organisms that have 10–100 times higher photosynthetic efficiency than higher plants (Ke, 2001). They use water as their electron source, sunlight as their energy source, and CO_2 as their carbon source. In turn, they produce oxygen, carbohydrates, proteins, and lipids (Ke, 2001). *Nannochloropsis oculata* are marine eustigmatophyceae containing up to 30–70% lipid by dry weight (Hodgson et al., 1991; Rodolfi et al., 2009). Additionally, *N. oculata* has a high biomass productivity reaching up to 3 g/L/day resulting

* Corresponding author.
E-mail address: pilon@seas.ucla.edu (L. Pilon).

0960-8524/$ - see front matter © 2013 Elsevier Ltd. All rights reserved.
http://dx.doi.org/10.1016/j.biortech.2013.03.058

in large lipid productivity (Briassoulis et al., 2010; Chen et al., 2011; Chisti, 2007). The lipids produced by microalgae are extracted and converted to biofuels such as biodiesel (Chisti, 2007).

Photosynthethic microalgae are typically cultivated in open ponds or enclosed photobioreactors (PBRs) (Chisti, 2007; Briassoulis et al., 2010). Light utilization efficiency of these PBRs is arguably the most important parameter affecting the overall efficiency of the biofuel production process. Thus, careful light transfer analysis must be conducted to design and optimize the light availability in PBRs and to operate them efficiently (Pilon et al., 2011). To do so, the spectral radiation characteristics of microalgae are necessary (Pilon et al., 2011).

This study specifically aims to measure the average absorption and scattering cross-sections and the total scattering phase function of *N. oculata* along with their complex index of refraction in the photosynthetically active radiation (PAR) region. It also aims to assess their dependency on the spectral distribution and the amplitude of the illuminance provided to the PBR during the microalgae growth.

1.1. Radiation harvesting pigments

Chlorophylls (chl) a, b, and c molecules are the primary pigments responsible for absorbing visible photons and transferring the charges to the reaction center. Carotenoids, on the other hand, can be divided into xanthophylls and carotenes (Ke, 2001). Carotenes are photosynthetic and absorb photons with wavelength corresponding to green and yellow colors and transfer the charges to chlorophyll molecules (Ke, 2001). Xanthophylls, on the other hand, act to protect the photosynthetic apparatus against excessive light (Ke, 2001). These photoprotective carotenoids quench poisonous free radicals and convert excess radiant energy into heat (Dubinsky and Stambler, 2000; Lubián et al., 2000; Gentile and Blanch, 2001). *N. oculata* contain the pigments chlorophyll *a*, β-carotene, and the xanthophylls violaxanthin and vaucherxanthin but lack chlorophyll *b* (Cohen, 1999).

Microalgae experience photoacclimation and chromatic acclimation in response to different incident irradiance and spectrum, respectively (Dubinsky and Stambler, 2000; Fisher et al., 1996; Gentile and Blanch, 2001). For example, they tend to increase their pigment concentrations in light-limited conditions. However, this may not lead to significant changes in their radiation characteristics as increasing the concentration of chlorophylls also decreases their *in vivo* specific absorption coefficient due to mutual shading of pigment molecules (Dubinsky and Stambler, 2000). The latter is partially responsible for what is known as the package effect corresponding to the non-linear relationship between cell pigment concentrations and cell absorption cross-section (Jonasz and Fournier, 2007). In addition, microalgae increase their photoprotective carotenoid concentration in response to large irradiance while reducing the amount of photosynthetic carotenoids through the so-called xanthophyll cycle (Dubinsky and Stambler, 2000; Lubián et al., 2000; Gentile and Blanch, 2001). The latter does not usually lead to changes in the overall carotenoid concentration as changes in the two types of carotenoids compensate each other (Dubinsky and Stambler, 2000; Lubián et al., 2000).

Moreover, photoacclimation and chromatic acclimation depend on the microalgae species. Even among *Nannochloropsis* species large difference in pigment expression exists. For example, Gentile and Blanch (2001) observed an 80% and 60% decrease in chl*a* and vioxanthin, respectively, in batch grown *Nannochloropsis gaditana* when the incident irradiance on a 250 ml flask was increased from 70 μmol/m^{2}s to 880 μmol/m^{2}s. Fisher et al. (1996) found that *Nannochloropsis* sp. grown under 30 μmol/m^{2}s, in continuous cultures, had a steady-state chlorophyll concentration 4.5 times larger than when grown under 650 μmol/m^{2}s. The low light-acclimated cells increased their number of photosynthetic units while the size of individual PSU remained constant. Lubián et al. (2000) demonstrated that *N. oculata* had lower concentrations of carotenoids canthaxanthin and astaxanthin and larger chlorophyll *a* concentration per cell compared with *N. gaditana* and *N. salina* for cultures grown under the same conditions. The pigment concentrations of *Nannochloropsis* sp. depend also on the PBR thickness and the initial cell concentration (Fisher et al., 1996; Zou and Richmond, 2000). Zou and Richmond (2000) showed that *Nannochloropsis* sp. had an order of magnitude larger steady-state chl*a* concentration per cell in cultures grown in 3 cm thick PBRs compared with those grown in 1 cm thick PBRs both exposed to 3000 μmol/m^{2}s. However, cells grown in 1 cm thick PBR had a larger carotenoid to chl*a* ratio. In addition, batch cultures of *Nannochloropsis* sp. with low initial cell density experienced a 5 day growth lag time while cultures with high initial cell concentration experienced no lag upon transfer to a PBR exposed to a photon flux density of 3500 μmol/m^{2}s.

1.2. Light transfer through microorganisms suspensions

Light transfer within absorbing, scattering, and non-emitting microalgal suspension in photobioreactors is governed by the radiative transport equation (RTE) expressed on a spectral basis as (Modest, 2003)

$$\hat{s} \cdot \nabla I_\lambda = -\kappa_\lambda I_\lambda(\hat{r}, \hat{s}) - \sigma_{s,\lambda} I_\lambda(\hat{r}, \hat{s}) + \frac{\sigma_{s,\lambda}}{4\pi} \int_{4\pi} I_\lambda(\hat{r}, \hat{s}_i) \Phi_{T,\lambda}(\hat{s}_i, \hat{s}) d\Omega_i \quad (1)$$

where $I_\lambda(\hat{r}, \hat{s})$ is the spectral radiation intensity in direction $\hat{s}$ at location $\hat{r}$ (in W/m^2·nm·sr) while κ_λ and $\sigma_{s,\lambda}$ are the effective absorption and scattering coefficients of the suspension (in 1/m). The total scattering phase function of the suspension $\Phi_{T,\lambda}(\hat{s}_i, \hat{s})$ represents the probability that radiation traveling in the solid angle $d\Omega_i$ around direction $\hat{s}_i$ is scattered into the solid angle $d\Omega$ around the direction $\hat{s}$ and is normalized such that

$$\frac{1}{4\pi} \int_{4\pi} \Phi_{T,\lambda}(\hat{s}_i, \hat{s}) d\Omega_i = 1. \quad (2)$$

The backward scattering ratio, denoted by b_λ, and the asymmetry factor, denoted by g_λ, for an axisymmetric phase function are defined as (Pilon et al., 2011)

$$b_\lambda = \frac{1}{2} \int_{\pi/2}^{\pi} \Phi_{T,\lambda}(\Theta) \sin\Theta \mathrm{d}\Theta \quad \text{and}$$
$$g_\lambda = \frac{1}{2} \int_0^{\pi} \Phi_{T,\lambda}(\Theta) \cos\Theta \sin\Theta \mathrm{d}\Theta \quad (3)$$

where Θ is the scattering angle between directions $\hat{s}_i$ and $\hat{s}$. The effective absorption coefficient κ_λ of a polydisperse microorganism suspension is related to the average absorption cross-sections, denoted by $\bar{C}_{abs,\lambda}$, as (Pilon et al., 2011)

$$\kappa_\lambda = \int_0^\infty C_{abs,\lambda}(d_s) N(d_s) \mathrm{d}d_s = \bar{C}_{abs,\lambda} N_T \quad (4)$$

where $N(d_s)$ is the number of cells per unit volume of suspension having diameter between d_s and $d_s + \mathrm{d}d_s$ and $C_{abs,\lambda}(d_s)$ is the absorption cross-section of a single spherical scatterer of diameter d_s. Here, N_T is the cell density defined as the total number of cells per m^3 of suspension. Similarly, the effective scattering coefficient can be written as

$$\sigma_{s,\lambda} = \int_0^\infty C_{sca,\lambda}(d_s) N(d_s) \mathrm{d}d_s = \bar{C}_{sca,\lambda} N_T \quad (5)$$

where $C_{sca,\lambda}(d_s)$ is the scattering cross-section of a single spherical scatterer of diameter d_s and $\bar{C}_{sca,\lambda}$ is the average scattering cross-section. Alternatively, the absorption and scattering coefficients can be expressed as the product of the average specific (or mass) absorption and scattering cross-sections $\bar{A}_{abs,\lambda}$ and $\bar{S}_{sca,\lambda}$ (in m^2/kg) and the microorganism mass concentration X (in kg/m^3) so that $\kappa_\lambda = \bar{A}_{abs,\lambda}X$ and $\sigma_{s,\lambda} = \bar{S}_{sca,\lambda}X$. Finally, the extinction coefficient β_λ (in 1/m) is given by $\beta_\lambda = \kappa_\lambda + \sigma_{s,\lambda}$.

The total scattering phase function of polydisperse microalgae cells $\Phi_{T,\lambda}(\Theta)$ can be estimated by averaging the scattering phase function of individual cells of diameter d_s, denoted by $\Phi_\lambda(d_s,\Theta)$, according to (Modest, 2003)

$$\Phi_{T,\lambda}(\Theta) = \frac{\int_0^\infty C_{sca,\lambda}(d_s)\Phi_\lambda(d_s,\Theta)N(d_s)\mathrm{d}d_s}{\int_0^\infty C_{sca,\lambda}(d_s)N(d_s)\mathrm{d}d_s} \tag{6}$$

Axisymmetric spheroidal microalgae with major and minor diameters a and b can be approximated as spheres with equivalent diameter d_s such that the surface area of the spheroid is equal to that of the equivalent sphere. Then, the equivalent diameter is expressed as (Lee et al., 2013)

$$d_s = \frac{1}{2}\left(2a^2 + 2ab\frac{\sin^{-1} e}{e}\right)^{1/2} \quad \text{where} \quad e = \frac{(\epsilon^2-1)^{1/2}}{\epsilon}. \tag{7}$$

Here, ϵ is the spheroid aspect ratio defined as $\epsilon = a/b$. The scatterer frequency distribution is denoted by $f(d_s)$ and defined as

$$f(d_s) = \frac{N(d_s)}{\int_0^\infty N(d_s)\mathrm{d}d_s} = \frac{N(d_s)}{N_T}. \tag{8}$$

Bidigare et al. (1987) and Pottier et al. (2005) used a predictive method for estimating the spectral absorption coefficient κ_λ by expressing it as a weighted sum of *in vivo* pigment specific absorption cross-sections $Ea_{\lambda,i}$ (in m^2/kg) according to

$$\kappa_\lambda = \sum_{i=1}^{n} Ea_{\lambda,i}c_i \tag{9}$$

where $(c_i)_{1\leqslant i\leqslant n}$ are the mass concentrations (in kg/m^3) of the cell's pigments. The specific absorption coefficient $Ea_{\lambda,i}$ (in m^2/kg) of chl*a*, *b*, and *c*, and β-carotene have been reported in the literature in the spectral range from 400 to 750 nm (Bidigare et al., 1990).

Gitelson et al. (2000) reported the average "specific mass absorption coefficient" (in m^2/kg) of *Nannochloropsis* sp. expressed as the ratio of the absorption coefficient κ_λ to the chlorophyll concentration c_{chla}. The authors used high density microalgae cultures with mass concentration X ranging from 1 to 8 kg/m^3 to measure the absorption coefficient in the spectral region from 400 to 750 nm. The microalgae were grown outdoors in 1–20 cm thick vertical flat panel photobioreactors using artificial seawater medium. The absorption coefficient κ_λ measurements were performed using an integrating sphere and were corrected for scattering errors according to the procedure outlined by Davies-Colley et al. (1986). Unlike what was expected, the specific absorption coefficient reported was not a linear function of chl*a* concentration for most wavelengths considered. The authors cited incomplete correction of the measurements for scattering errors and large noise as the cause for the non-linearity (Gitelson et al., 2000). We speculate that multiple scattering through such dense suspensions was also in part responsible for these observations.

The present study reports the radiation characteristics of *N. oculata* consisting of the total scattering phase function $\Phi_{T,\lambda}(\Theta)$ at 633 nm, the average absorption and scattering cross-sections $\bar{C}_{abs,\lambda}$ and $\bar{C}_{sca,\lambda}$ between 350 and 750 nm of microalgae grown using white fluorescent light or red LEDs under various illuminances. The corresponding spectral complex index of refraction was also retrieved from the measured average absorption and scattering cross-sections and size distribution. Finally, the measured spectral absorption coefficient was compared with that predicted by Eq. (9) using the experimentally measured pigment concentrations.

2. Methods

2.1. Microalgae cultivation and sample preparation

Microalgae species *N. oculata* UTEX 2164 was purchased from UTEX Austin, TX. Table 1 summarizes the experimental and growth conditions used to cultivate the microalgae to measure their radiation characteristics. The microalgae were cultivated in Erdshriber's medium in 2.0 cm thick, 200 ml flat culture bottles fitted with vented caps exposed to (i) an illuminance of 2000 lux provided by fluorescent light bulbs (GroLux by Sylvania, USA) or to (ii) an illuminance of 2000, 5000, or 10,000 lux provided by red LEDs (C503B-RAN Cree, USA) with peak wavelength at 630 nm and spectral bandwidth of 30 nm. The conversion between photon flux density and illuminance for the red LEDs and the white fluorescent light source were 47.5 and 33 lux per 1 μmol photon/m^2s, respectively. Mixing of the suspension was performed manually twice a day. The Erdshriber medium had the following composition (per liter of pasteurized seawater): $NaNO_3$ 0.2 g, Na_2HPO_4 0.02 g, $Na_2EDTA{\cdot}2H_2O$ 7.5 mg, $CoCl_2{\cdot}6H_2O$ 0.02 mg, $FeCl_3{\cdot}6H_2O$ 0.97 mg, $ZnCl_2$ 0.05 mg, $MnCl_2{\cdot}4H_2O$ 0.41 mg, $Na_2Mo_4{\cdot}2H_2O$ 0.04 mg, and vitamin B12 0.135 mg, and 50 ml soil water: GR+ medium.

Some microalgae were also grown in 1 cm pathlength PBRs in artificial seawater medium. The PBR was exposed from both sides to red LEDs with illuminance of 2 × 2500 or 2 × 5000 lux. The artificial seawater medium (ASWM) used had the following composition (per liter of deionized water): NaCl 18 g, $MgSO_4{\cdot}7H_2O$ 2.6 g, KCl 0.6 g, $NaNO_3$ 1 g, $CaCl_2{\cdot}2H_2O$ 0.3 g, KH_2PO_4 0.05 g, NH_4Cl 0.027 g, $Na_2EDTA{\cdot}2H_2O$ 0.03 g, H_3BO_3 0.0114 g, $FeCl_3{\cdot}6H_2O$ 2.11 mg, $MnSO_4{\cdot}H_2O$ 1.64 mg, $ZnSO_4{\cdot}7H_2O$ 0.22 mg, $CoCl_2{\cdot}6H_2O$ 0.048 mg, and vitamin B12 0.135 mg. These cultures were continuously injected with 2 vol.% air/CO_2 at 7 ml/min at STP and were placed on an orbital shaker rotating at 95 rpm. Fig. 1 shows the normalized emission spectrum of both light sources. It also shows the mass absorption cross-sections $Ea_{\lambda,i}$ of photosynthetic pigment chl*a* as well as carotenoids (Bidigare et al., 1990).

Samples used to perform the measurements were taken during the exponential growth phase. Additionally, to avoid absorption and scattering by the growth medium, the microalgae were centrifuged at 10,000 rpm (6500 g) for 2 min and washed twice with phosphate buffer saline (PBS) solution and suspended in PBS. The

Table 1
Summary of experimental conditions used to measure the radiation characteristics of *N. oculata* after 6 days of growth with initial concentration X = 0.01 kg/m^3.

Light source	Illuminance (lux)	Medium	Aeration	Reactor thickness (cm)	Concentration (kg/m^3)	Mixing
White fluorescent	2000	Erdshriber	Vented caps	2.0	0.158	Manually twice a day
Red LEDs	2000	Erdshriber	Vented caps	2.0	0.159	Manually twice a day
Red LEDs	5000	Erdshriber	Vented caps	2.0	0.084	Manually twice a day
Red LEDs	10,000	Erdshriber	Vented caps	2.0	0.090	Manually twice a day
Red LEDs	2 × 2500	Artificial seawater	2% v/v air/CO_2	1.00	1.33	Orbital shaker (95 rpm)
Red LEDs	2 × 5000	Artificial seawater	2% v/v air/CO_2	1.00	1.23	Orbital shaker (95 rpm)

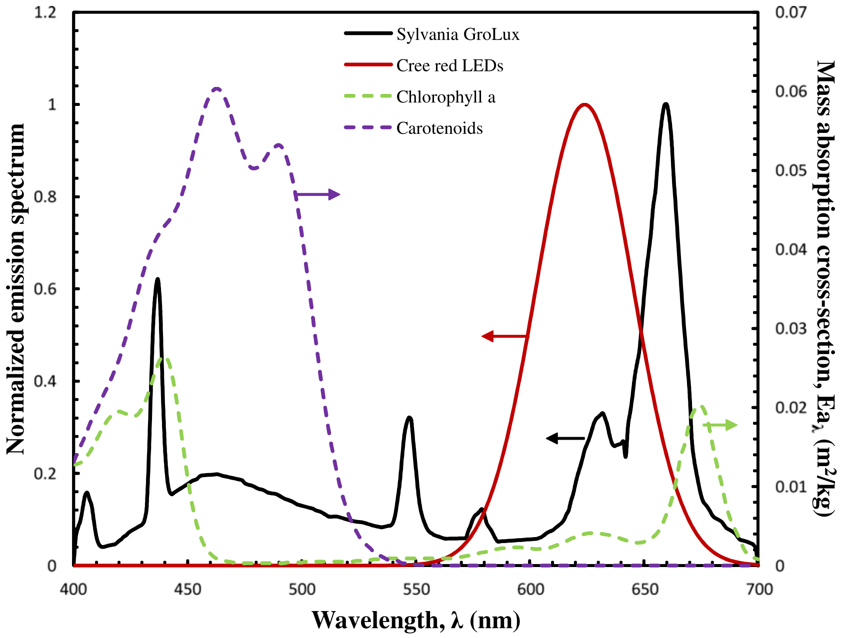

Fig. 1. Normalized emission spectrum of Sylvania GroLux white fluorescent light source and Cree red LEDs used for *N. oculata* cultivation along with *in vivo* absorption cross-sections (in m^2/mg) of chlorophyll *a*, carotenoids (Bidigare et al., 1990). (For interpretation of the references to color in this figure legend, the reader is referred to the web version of this article.)

cell size distribution was measured using 2D microscope images captured using a Leica LMIL microscope (Leica Microsystems, USA) connected to a CCD camera (Spot Insight model 4.2, USA). The image analysis software imageJ was used to manually measure the major and minor diameters of individual cells approximated as axisymmetric spheroids. The data was used to determine the equivalent diameter d_s and the size and frequency distributions $N(d_s)$ and $f(d_s)$.

Microorganism mass concentration X and cell density N_T were determined using calibration curves relating them to the optical density (OD) of the microalgae suspension at 750 nm. The normal–normal transmittance T_λ and the $OD_\lambda = -lnT_\lambda$ were measured for several concentrations of microalgae at 750 nm in disposable polystyrene cuvettes with pathlength 1 cm using a Fourier transform infrared spectrometer (FTIR) (ThermoNicolet Magna-IR 560). The mass concentration X for five different microalgae dilutions was obtained by filtering the cells through washed and dried 0.45 nm pore size cellulose membrane filters (HAWP-04700 by Millipore, USA) followed by drying at 60 °C in a vacuum oven overnight. The dried filters with the dry cells were weighted immediately after being removed from the oven using a precision balance (model AT261 by Delta Range Factory, USA) with a 0.01 mg precision. The cell density N_T in each dilution was counted using a 20 μm deep Petroff-Hausser counting chamber (Hausser Scientific model 3400, USA). The resulting calibration curves were $X = 0.207OD_{750}$ and $N_T = 1.72 \times 10^{14}OD_{750}$ with correlation coefficient R^2 of 0.99 for both calibrations. Here, X and N_T are expressed in dry kg/m^3 and number of cells/m^3 of suspension, respectively.

2.2. Experiments

2.2.1. Assumptions

The following assumptions were made when estimating the average absorption and scattering cross-sections as well as the effective optical properties of the microalgae: (1) The microorganisms were well mixed and randomly oriented. (2) The microalgae were assumed to be homogeneous with an effective complex index of refraction $m_\lambda = n_\lambda + ik_\lambda$. (3) They were also assumed to be axisymmetric spheroids and treated as spheres. (4) Single scattering prevailed since we considered low concentration suspensions. (5) The total scattering phase function of the suspension had azimuthal symmetry and was only a function of the polar angle Θ. (6) As a first order approximation, the scattering phase function was assumed to be constant over the PAR region.

2.2.2. Scattering phase function

The total scattering phase function was measured at 633 nm by a polar nephelometer. The experimental setup and data analysis have previously been reported by Berberoğlu et al. (2008) and need not be repeated. Due to probe interference with the incident laser beam, it was only possible to collect measurements for scattering angles Θ up to 170°. Thus, in order to accurately determine b_λ, it was computed based on the following expression (Modest, 2003)

$$b_\lambda = 1 - \frac{1}{2}\int_0^{\pi/2} \Phi_{T,\lambda}(\Theta)\sin\Theta d\Theta \tag{10}$$

The apparatus and data analysis were validated by successfully comparing the measured scattering phase function of monodispersed latex spheres of 5 μm diameter and predictions from Lorentz–Mie theory using the complex index of refraction of latex at 633 nm as $m_{633} = 1.5823 + i4.5 \times 10^{-4}$ (Ma et al., 2003) (not shown).

2.2.3. Absorption and scattering cross-sections

The extinction coefficient β_λ was estimated from normal–normal transmittance measurements between 350 and 750 nm using UV–vis-NIR spectrophotometer (Shimadzu, USA, model UV-3101PC). The microalgae suspensions were diluted to ensure single scattering. The absorption coefficient κ_λ was determined from normal-hemispherical measurements performed between 350 and 750 nm using an integrating sphere (Shimadzu ISR-3100) attached to the UV–vis-NIR spectrophotometer (Berberoğlu et al., 2008). The results for both measurements were corrected for scattering errors and the setup and data analysis was validated according to the analysis presented by Berberoğlu et al. (2008). Measurements were performed for three different concentrations to assess their repeatability and the validity of Eqs. (4)–(6) as well as to estimate the average cross-sections $\bar{C}_{abs,\lambda}$ and $\bar{C}_{sca,\lambda}$ and the associated experimental uncertainty.

2.3. Retrieving the microalgae effective complex index of refraction

An inverse method combined with Lorentz–Mie theory was used to retrieve the complex index of refraction from (i) the measured average absorption and scattering cross-sections $\bar{C}_{abs,\lambda}$ and $\bar{C}_{sca,\lambda}$, (ii) the cell equivalent diameter distribution $N(d_s)$, and (iii) the spectral refraction index of PBS reported by Zhernovaya et al. (2011). General purpose genetic algorithm code PIKIA (Charbonneau, 1995) was used with a maximum of 30 generations each with a population of 120 individuals to retrieve the refraction and absorption indices for 41 wavelengths between 350 and 750 nm in 10 nm increments. This method was recently developed and described in detail by Lee et al. (2013).

2.4. Pigment concentrations

Chlorophyll *a* and total carotenoid contents were determined spectrophotometrically using 24 h extraction in methanol as it is most efficient at extracting pigments from microalgae (Wellburn, 1994). Note that this method estimates the total carotenoid concentration in the cells and not that of a specific carotenoid. A 2 ml sample of microalgae culture was centrifuged for 2 min at 10,000 rpm (6500 g) and the medium discarded. Then, 3 ml of pure methanol was added to the cell pellets and vortexed for 1 min. The samples were left in a dark room for 24 h at approximately 22 °C to ensure maximum pigment extraction. The samples were then centrifuged and the supernatant collected and transferred to 1 cm pathlength polystyrene cuvettes for OD measurements at 480, 666, and 750 nm. The pigment extractions were performed in duplicates and the measurements were repeated three times and averaged. The cell pellets were checked for complete extraction by performing double extractions.

The chlorophyll *a* concentration (in μg/m^3 of suspension) was calculated using the correlation (Wellburn, 1994)

$$c_{chla} = 15.65(\mathrm{OD}_{666} - \mathrm{OD}_{750})\,v/Vl \tag{11}$$

where V is the microalgae sample volume (in m^3), v is the volume of solvent (in m^3), and l is the cuvette pathlength (in cm). Similarly, the total carotenoid concentration (in µg/m^3) was calculated according to (Strickland and Parsons, 1968)

$$c_{x+c} = 4(\mathrm{OD}_{480} - \mathrm{OD}_{750})\,v/Vl \tag{12}$$

Pigment mass fraction (in kg of pigment/kg of dry cell) was estimated as the ratio of pigment concentration to dry mass concentration X, i.e., $w_{chla} = c_{chla}/X$ and $w_{x+c} = c_{x+c}/X$ (Andersen, 2005).

3. Results and discussion

3.1. Mass concentration

All measurements were performed after 6 days of growth in batch mode with an initial mass concentration of 0.01 kg/m^3. The mass concentrations of microalgae at the time the optical measurements were performed are reported in Table 1. The microalgae in PBRs injected with 2 vol.% CO_2 showed the largest increase in mass concentration, after 6 days, reaching X = 1.33 kg/m^3 for microalgae in PBRs exposed to 2500 lux red LEDs from both sides. On the other hand, the microalgae grown in vented caps (i.e., without CO_2 injection) exposed to light from a single side showed an order of magnitude lower mass concentration. For example, X reached 0.158 kg/m^3 for microalgae grown under 2000 lux of red LEDs or white fluorescent light, after 6 days. It fell to 0.084 and 0.090 kg/m^3 when grown under 5000 and 10,000 lux, respectively.

3.2. Size distribution

Fig. 2 shows a histogram of the equivalent diameter frequency distribution $f(d_s)$ of the microalgae calculated using Eq. (7) with bins 0.1 µm in width. This distribution was estimated from at least 300 cells for each microalgae suspension grown with six different incident spectra or illuminances. The equivalent cell diameter and the cell aspect ratio did not vary appreciably for the different illumination conditions considered. In all cases, the average equivalent diameter was between 2.52 and 2.63 µm and the standard deviation was 0.35–0.45 µm.

3.3. Scattering phase function

Fig. 3 shows the measured total scattering phase functions at 633 nm of *N. oculata* suspension grown under 2000 lux white and red light sources. As expected, given the large equivalent cell diameter compared with the wavelength, scattering was mainly in the forward direction with asymmetry factor found to be $g_{633} = 0.986$ at 633 nm for microalgae grown under either light sources. Furthermore, the backward scattering ratio was very small and equal to $b_{633} = 0.0013$ and $b_{633} = 0.0019$ for microalgae grown using white light and red LEDs, respectively.

3.4. Absorption and scattering cross-sections

Figs. 4a and b show the measured absorption and scattering cross-sections, in the spectral region from 350 to 750 nm, for *N. oculata* grown under (i) white light with an illuminance of 2000 lux, (ii) red LEDs with an illuminance of 2000, 5000, and 10,000 lux on one side of a 2 cm thick flat culture bottles and (iii) red LEDs with 2500 and 5000 lux on both sides of the 1 cm thick PBR. The results for $\bar{C}_{abs,\lambda}$ and $\bar{C}_{sca,\lambda}$ shown in Fig. 4 represent the arithmetic mean of the cross-sections measured three times for each of the three different concentrations considered. The error bars correspond to 95% confidence interval. The relatively small error bars established that the absorption and scattering cross-sections were independent of microorganism cell density as assumed in Eqs. (4) and (5). It also confirms that multiple scattering was negligible for the cell densities considered. Furthermore, it is evident that scattering dominated over absorption for all wavelengths in the PAR region, i.e., $\bar{C}_{sca,\lambda} > \bar{C}_{abs,\lambda}$. The absorption peaks for *in vivo* chl*a* were apparent at 436 nm, 630 nm, and 676 nm (Ke, 2001) while that of carotenoids was observed at 480 nm (Ke, 2001). Note that the chl*a* peak at 630 nm is usually concealed by absorption peak of chl*b* in green microalgae (Berberoğlu et al., 2008, 2009) which is lacking in *N. oculata*.

The absorption and scattering cross-sections for *N. oculata* grown under 2000 lux of white and red light sources fell within their experimental uncertainty ranges for all wavelengths considered. This indicates that no chromatic adaptation occurred in the cells despite the different emission spectra of the fluorescent white light and the red LEDs (Fig. 1). In addition, the absorption and scattering cross-sections of *N. oculata* grown under red LEDs providing illuminance of 2000, 5000, and 10,000 lux featured slight variations that fell within their experimental error bars for most wavelengths considered. The slight differences could be attributed to small variation in pigment concentrations, in particular around 480 nm corresponding to absorption peaks of photoprotective carotenoids (Bidigare et al., 1990).

By contrast, *N. oculata* grown in PBR exposed to red light from both sides and injected with 2 vol.% CO_2/air mixture featured smaller absorption cross-sections than those grown in the thicker bioreactors exposed to light from only one side. This may be explained by the fact that the microalgae had reached significantly larger concentration and may have depleted a significant amount

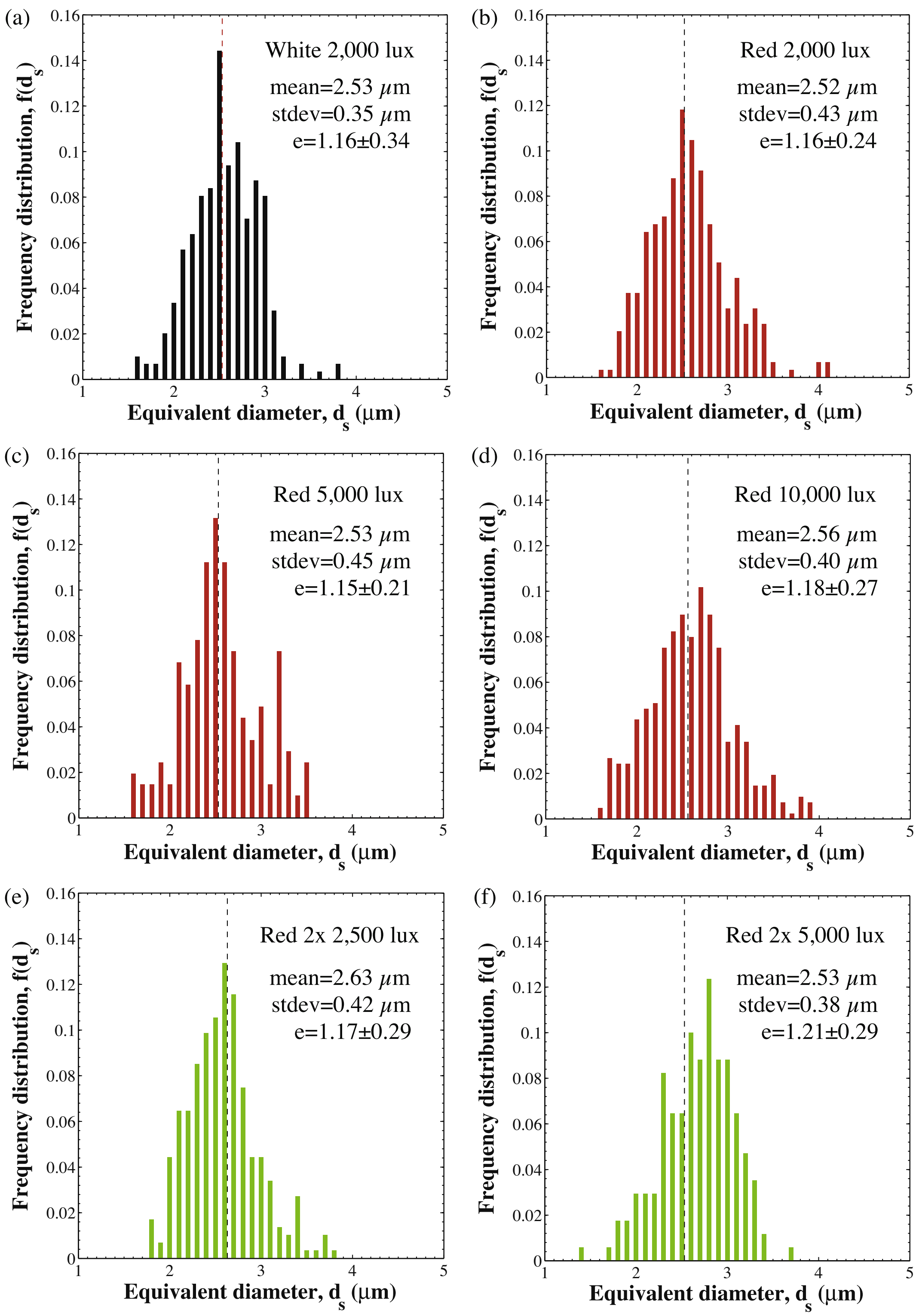

Fig. 2. Histogram of frequency distribution $f(d_s)$ of the equivalent diameter d_s of *N. oculata* grown under (a) white light at 2000 lux and red LEDs at (b) 2000 lux, (c) 5000 lux, (d) 10,000 lux, (e) 2500 lux from two side, and (f) 5000 lux from two sides. The equivalent diameter was calculated from the measured major and minor diameters using Eq. (7). At least 300 cells were measured for each batch. (For interpretation of the references to color in this figure legend, the reader is referred to the web version of this article.)

of nutrients initially available in the medium. In fact, nitrate limited conditions can stunt biomass production in *Nannochloropsis* sp. and cause a decrease in cell pigment concentrations leading to reduced absorption cross-section $\bar{C}_{abs,\lambda}$ (Cohen, 1999). Furthermore, the microalgae exposed to an illuminance of 5000 lux from both sides featured larger absorption cross-sections than those exposed to 2500 lux from both sides. This could be attributed to the fact that microalgae grown with the 2 × 2500 lux were harvested at a later stage of their growth and their mass concentration X had reached 1.33 kg/m^3 compared with 1.23 kg/m^3 for *N. oculata* grown under 2 × 5000 lux. In fact, nutrient availability in the medium can be estimated by stoichiometric calculation. The exact elemental composition of *N. oculata* was not available in the literature. However, microalgae elemental composition does not

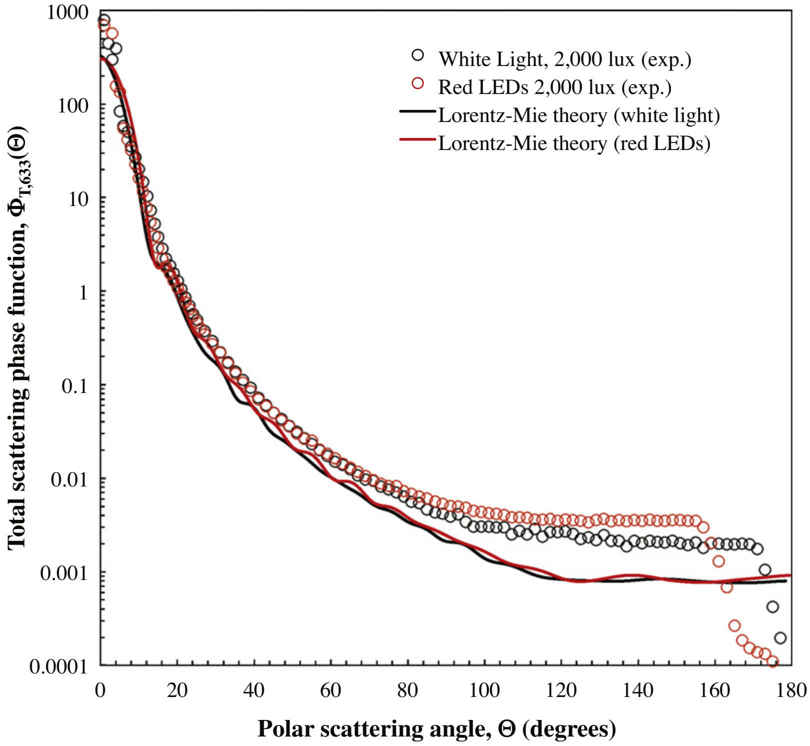

Fig. 3. Total scattering phase function $\Phi_{T,633}(\Theta)$ of *N. oculata* at 633 nm measured experimentally using a polar nephelometer for microalgae grown under white light and red LEDs with illuminance of 2000 lux. The experimental phase functions were compared with predictions by Eq. (6) using (i) Lorentz–Mie theory, (ii) the measured equivalent diameter distribution $N(d_s)$, and (iii) the retrieved complex index of refraction at 633 nm $m_{633} = 1.3675 + i9.997 \times 10^{-4}$. (For interpretation of the references to color in this figure legend, the reader is referred to the web version of this article.)

vary appreciably between different species and has been reported to be composed of 8–12% nitrogen (N) and 0.8–1.5% phosphorus (P) by weight (Parsons et al., 1961; Williams and Laurens, 2010; Van Vooren et al., 2012). Assuming a 10% N and 1% P composition by weight for *N. oculata* cells suggests that the culture experienced a phosphate limitation at a biomass concentration of 1.14 g/L and a nitrogen limitation around 1.52 g/L. In addition, the average scattering cross-section $\bar{C}_{sca,\lambda}$ of the microalgae grown with 2×2500 lux was larger than that of microalgae grown with 2×5000 lux. This may be due to their larger mean equivalent diameter of 2.63 μm instead of 2.53 μm (Jonasz and Fournier, 2007). Indeed, Lorentz–Mie theory estimates that the scattering cross-section $C_{sca,550}$ of cells (m_{550}=1.37 + i2 $\times 10^{-4}$) with diameter 2.53 and 2.63 μm suspended in PBS were 3.17×10^{-12} m^2 and 3.68×10^{-12} m^2, respectively. In other words, the scattering cross-section increased by 14% as the cell radius increased by 4%.

Finally, the average scattering cross-section $\bar{C}_{sca,\lambda}$ of *N. oculata* was two orders of magnitude smaller than those of significantly larger green microalgae such as *Botryococcus braunii* (d_s = 9–15 μm) and *Chlorococcum littorale* (d_s = 6–12 μm) (Berberoğlu et al., 2009). This is consistent with light scattering theory suggesting that the scattering cross-section increases with the size parameter $\chi = \pi d_s/\lambda$ (Jonasz and Fournier, 2007).

3.5. Real and imaginary parts of the complex index of refraction

Figs. 5a and b show the retrieved refraction and absorption indices of *N. oculata* grown under (i) white light with illuminance of 2000 lux, (ii) red LEDs with illuminance of 2000, 5000, and 10,000 lux on one side of a 2 cm thick flat culture bottles and (iii) red LEDs with 2×2500 and 2×5000 lux on both sides of the 1 cm thick PBR with CO_2 injection. The effective refractive index was nearly identical for microalgae grown with white and red light under any illuminance delivered on one or both sides of the PBR. In fact, the relative difference in the effective refraction index n_λ was less than 0.1% for all growth conditions and wavelengths considered. These observations confirm that differences in scattering cross-section $\bar{C}_{sca,\lambda}$, previously discussed, were likely due to differences in size. In addition, the refraction index n_λ ranged from 1.365 to 1.376 and was comparable to the effective refraction indices reported for other microalgae (Lee et al., 2013; Jonasz and Fournier, 2007). Here also, n_λ featured dips at wavelengths corresponding to peaks observed in the effective absorption index k_λ. These dips can be attributed to oscillator resonance around the peak absorption wavelengths as predicted by the Helmholtz–Kettler theory describing the relationship between n_λ and k_λ (Jonasz and Fournier, 2007). Note that the amplitude of the resonance in n_λ decreased as the absorption peaks in k_λ weakened.

Fig. 5b indicates that the effective absorption index k_λ ranged from 0 to 4.32×10^{-3} with peaks at 436, 480, 630, and 676 nm. It was identical for *N. oculata* grown in culture bottles with vented caps under white light and red LEDs with illuminance of 2000 lux and under red LEDs with 5000 and 10,000 lux. In addition, the absorption index of microalgae grown in the 1 cm thick PBRs with 2×2500 lux red LEDs and CO_2 sparging was on average 76% lower than that of microalgae grown with 5000 lux red LEDs exposed from one side without CO_2 injection. Similarly, microalgae grown in the 1 cm thick PBR with 2×5000 lux red light and CO_2 injection had absorption index 36% smaller than those grown under red light at 10,000 lux on one side without CO_2 injection. As previously suggested, the lower absorption index in the CO_2 sparged PBRs illuminated on both sides could be attributed to the lower pigment content of the cells caused by nutrient deficient conditions.

3.6. Lorentz–Mie scattering phase function

Fig. 3 displays the total scattering phase function $\Phi_{T,633}(\Theta)$ of *N. oculata* grown under 2000 lux predicted by Eq. (6) where $\Phi_\lambda(d_s,\Theta)$

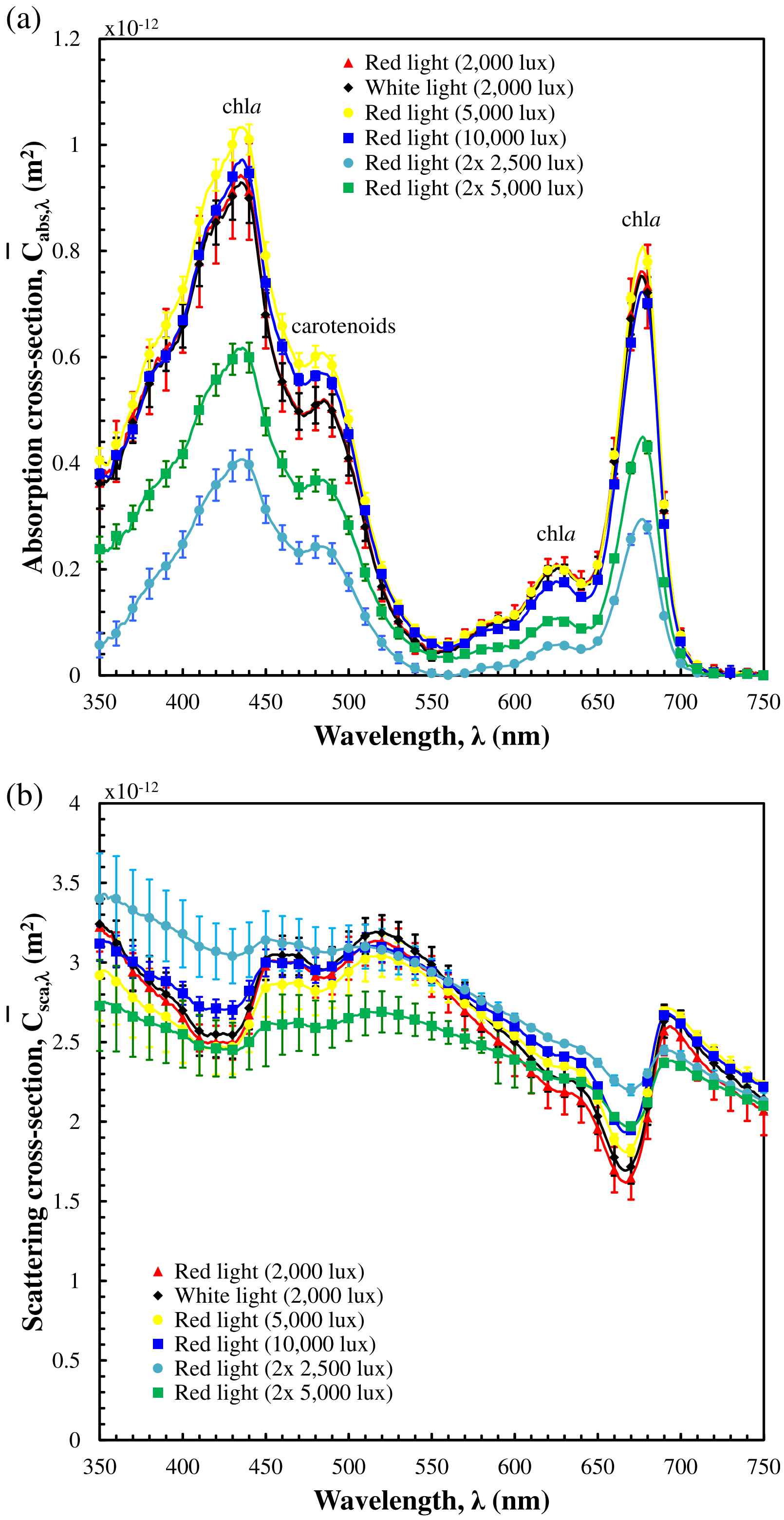

Fig. 4. Average spectral (a) absorption $\bar{C}_{abs,\lambda}$ and (b) scattering $\bar{C}_{sca,\lambda}$ cross-sections of *N. oculata* grown with fluorescent white light with illuminance of 2000 lux and red LEDs with illuminance ranging from 2000 to 10,000 lux. Absorption peaks of chl*a* were observed at 436, 630, and 676 nm and that of carotenoids at 480 nm. (For interpretation of the references to color in this figure legend, the reader is referred to the web version of this article.)

was predicted by Lorentz–Mie theory using (i) the retrieved complex index of refraction at 633 nm $m_{633} = 1.3675 + i9.997 \times 10^{-4}$, (ii) the refraction index of PBS taken as $n_{PBS,633} = 1.334$ (Zhernovaya et al., 2011), and (iii) the measured equivalent diameter distribution $N(d_s)$. The backward scattering ratio b_{633} was estimated from Lorentz–Mie theory to be 0.0006 for microalgae grown using either light source. This value should be compared with experimental measurements of b_{633} of 0.0013 and 0.0019 for white and red incident light at 2000 lux, respectively. More importantly, the asymmetry factor g_{633} estimated from Lorentz–Mie theory for

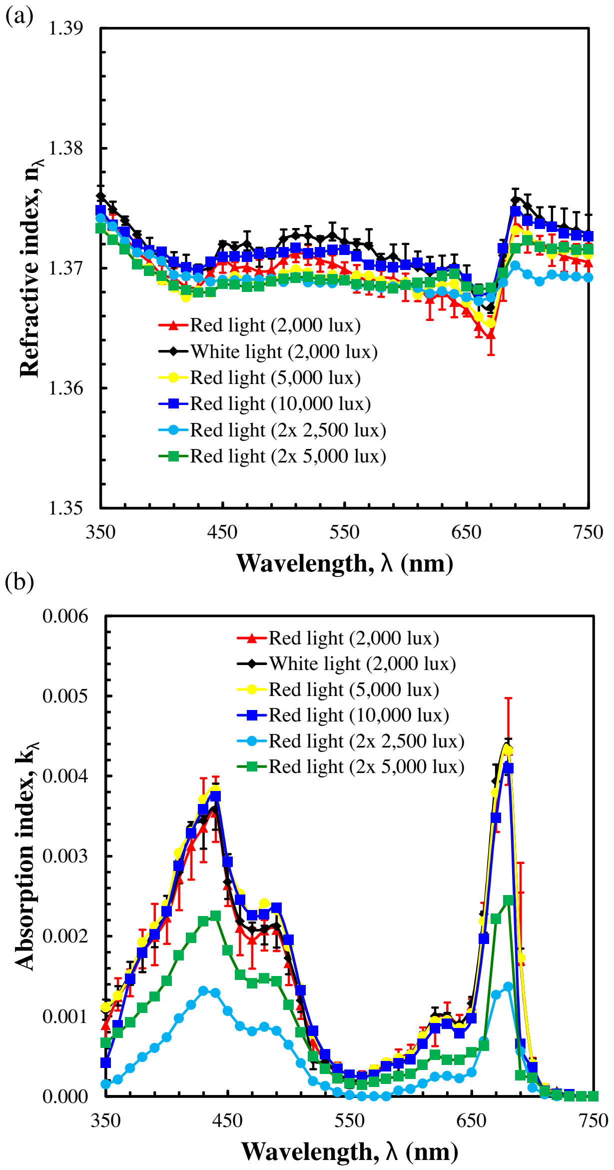

Fig. 5. Spectral (a) refraction n_λ and (b) absorption k_λ indices of *N. oculata* retrieved using Lorentz–Mie theory for microalgae grown (i) in culture bottles with vented caps illuminated on one side with fluorescent white light with illuminance of 2000 lux and red LEDs with illuminance ranging from 2000 to 10,000 lux and (ii) in 1 cm thick PBR injected with 2 vol.% CO_2 and illuminated on both sides by 2 × 2500 lux and 2 × 5000 lux. (For interpretation of the references to color in this figure legend, the reader is referred to the web version of this article.)

microalgae grown under both light sources was 0.988 compared with 0.986 measured experimentally.

Furthermore, the asymmetry factor g_λ was estimated from Lorentz–Mie theory over the spectral range from 350 to 750 nm using the equivalent diameter distribution $N(d_s)$ and the spectral refraction and absorption indices retrieved for *N. oculata* grown under 2000 lux (Figs. 5a and b). It was found to be nearly independent of wavelength over the PAR region as it only varied between 0.9878 and 0.9884. This confirms Assumption 6 made when correcting normal–normal and normal–hemispherical transmittances for forward scattering.

3.7. Pigment concentrations

Table 2 summarizes the chlorophyll *a* and total carotenoid mass fractions in wt.% extracted from *N. oculata* for each light source and illuminance considered. The extracted chl*a* mass fraction was w_{chla} = 2.25 ±0.04 wt.% and 2.21 ± 0.16 wt.% for *N. oculata* grown using 2000 lux white light and red LEDs, respectively. Their respective total carotenoid mass fraction w_{x+c} was 0.73 ± 0.01 wt.% and 0.72 ± 0.07 wt.%. Overall, there was no statistically significant difference in pigment concentrations between the batches grown under 2000 lux using white light or red LEDs indicating that no chromatic adaptation occurred. These pigment concentrations and dry mass fractions were also consistent with those previously reported in the literature for *N. oculata* (Gitelson et al., 2000; Simionato et al., 2011).

Table 2
Chlorophyll *a* and total carotenoid mass fractions (%) and chlorophyll *a* to carotenoid ratio extracted from *N. oculata* grown under various light sources and illuminances summarized in Table 1.

Light source	Illuminance (lux)	Chlorophyll *a* (wt.%)	Total carotenoid (wt.%)	w_{x+c}/w_{chla}
White	2000	2.25 ± 0.04	0.73 ± 0.01	0.32
Red	2000	2.21 ± 0.16	0.72 ± 0.07	0.32
Red	5000	2.46 ± 0.12	0.56 ± 0.06	0.23
Red	10,000	2.08 ± 0.01	0.43 ± 0.01	0.21
Red	2 × 2500	0.28 ± 0.002	0.45 ± 0.01	1.61
Red	2 × 5000	0.549 ± 0.03	0.23 ± 0.06	0.43

The chlorophyll *a* and total carotenoid mass fractions of microalgae grown under red LEDs with different incident illuminances showed trends similar to those observed in their absorption cross-sections (Fig. 4a). There were no statistically significant changes in the measured pigment concentrations. Larger carotenoid mass fraction has been reported in *Nannochloropsis* sp. grown under larger irradiances (Cohen, 1999). However, Lubián et al. (2000) showed this effect to be significant in *N. salina* while the increase in zeaxanthin, astaxanthin, and antheraxantin in *N. oculata* were less pronounced and coincided by reduction in vioxanthin, thus maintaining an approximately constant total carotenoid mass fraction. The ratio of carotenoid to chlorophyll content is often cited as the measure of stress the culture is experiencing. Van Vooren et al. (2012) showed that the ratio of carotenoid to chlorophyll *a* in *N. oculata* increased during nitrogen starvation and exceeded unity. Similarly, in the PBRs injected with CO_2 and illuminated from both sides, this ratio was larger compared with microalgae grown in the thicker PBR illuminated from one side without CO_2 injection, as summarized in Table 2. In fact, it reached 1.61 for the microalgae grown in PBR exposed to 2 × 2500 lux further supporting the assertion of nutrient starvation in this culture.

Moreover, Table 2 indicates that microalgae grown in the 1 cm thick CO_2-sparged PBRs exposed to red LEDs on both sides had pigment mass fractions one order of magnitude lower than those grown in the thicker PBR exposed to light from only one side. Furthermore, *N. oculata* grown exposed to 2 × 2500 lux contained lower chl*a* and carotenoids mass fractions than those exposed to 2 × 5000 lux, under otherwise similar conditions. This can be attributed to more severe nutrient deficient conditions in the PBRs exposed to 2 × 2500 lux where microalgae concentration was the largest.

3.8. Model validation

Fig. 6 shows the absorption coefficient κ_λ of a microalgae culture with a mass concentration $X = 0.10$ kg/m^3 measured experimentally for *N. oculata* grown under 2000 lux using white light and that predicted by Eq. (9) using the experimentally measured pigment concentrations c_{chla} and c_{x+c}. The average relative error between experimental measurements and predictions of κ_λ by Eq. (9) was 36% over the PAR region. The relative error was 11% and 28% at 436 nm and 676 nm corresponding to chl*a* absorption peaks. At

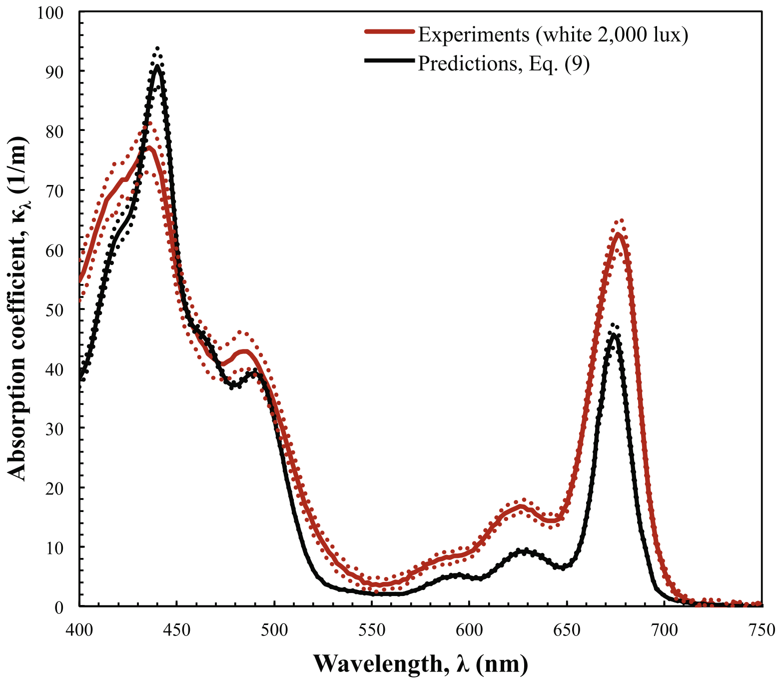

Fig. 6. Comparison of the experimentally measured absorption coefficient of *N. oculata* grown with 2000 lux white fluorescent light with mass concentration $X = 0.10$ kg/m^3 and that predicted by Eq. (9) using the measured pigment concentrations $c_{chla} = 2.25 \times 10^{-3}$ kg/m^3, $c_{x+c} = 1.30 \times 10^{-3}$ kg/m^3. The dotted lines correspond to 95% confidence intervals. (For interpretation of the references to color in this figure legend, the reader is referred to the web version of this article.)

these wavelengths, the predicted mass absorption cross-section featured sharper absorption peaks than those experimentally measured. This was also observed for other microalgae species (Lee et al., 2013). The flattening of the absorption peaks observed experimentally may be due to the so-called "package effect" (Jonasz and Fournier, 2007). In other words, pigments display a different absorption cross-section once they are packaged inside a cell. This is due to the non-linear dependence of absorption on (i) pigment concentrations, (ii) cell refractive index, (iii) cell size, and (iv) pigment location within the cell (Jonasz and Fournier, 2007). This suggests that simple superposition of the individual pigment's absorption cross-sections, as suggested by Eq. (9), represents a first order approximation and may not be adequate to accurately predict the mass absorption cross-section of microalgae.

4. Conclusions

This study measured the absorption and scattering cross-sections and optical properties over the PAR region of *N. oculata* grown under white light and red LEDs with illuminance ranging from 2000 to 10,000 lux. The microalgae average equivalent diameter ranged from 2.52 to 2.63 μm. Their cross-sections and optical constant were statistically identical over most of the PAR region. Other *N. oculata* grown in 2 vol.% CO_2 injected PBRs featured lower pigment concentrations and significantly smaller absorption cross-section and absorption index due to nutrient limited growth conditions. By contrast, the refraction index was identical for all conditions considered.

Acknowledgements

This research was supported in part by the National Science Foundation IGERT program Clean Energy for Green Industry at UCLA (DGE-0903720). The data presented in this paper are available for download on our research group website (Pilon, 2013).

References

Andersen, R., 2005. Algal Culturing Techniques. Elsevier/Academic Press, San Diego, CA.

Williams, P.J. le B., Laurens, L., 2010. Microalgae as biodiesel and biomass feedstocks: review and analysis of the biochemistry energetics and economics. Energy Environmental Science 3, 554–590.

Berberoğlu, H., Gomez, P.S., Pilon, L., 2009. Radiation characteristics of *Botryococcus braunii*, *Chlorococcum littorale* and *Chlorella* sp. used for fixation and biofuel production. Journal of Quantitative Spectroscopy and Radiative Transfer 110 (17), 1879–1893.

Berberoğlu, H., Pilon, L., Melis, A., 2008. Radiation characteristics of *Chlamydomonas reinhardtii* CC125 and its truncated chlorophyll antenna transformants *tla1 tlaX* and *tla1-CW+*. International Journal of Hydrogen Energy 33 (22), 6467–6483.

Bidigare, R.R., Ondrusek, M.E.E., Morrow, J.H.H., Kiefer, D.A.A., 1990. *In-vivo* absorption properties of algal pigments. In: Proceedings of SPIE, vol. 1302. pp. 290–302.

Bidigare, R.R., Smith, R.C., Baker, K.S., Marra, J., 1987. Oceanic primary production estimates from measurements of spectral irradiance and pigment concentrations. Global Biogeochemical Cycles 1 (3), 171–186.

Briassoulis, D., Panagakis, P., Chionidis, M., Tzenos, D., Lalos, A., Tsinos, C., Berberidis, K., Jacobsen, A., 2010. An experimental helical-tubular photobioreactor for continuous production of *Nannochloropsis* sp. Bioresource Technology 101 (17), 6768–6777.

Charbonneau, P., 1995. Genetic algorithms in astronomy and astrophysics. The Astrophysical Journal Supplement Series 101, 309–334.

Chen, C., Yeh, K., A, R., Lee, D., Chang, J., 2011. Cultivation photobioreactor design and harvesting of microalgae for biodiesel production: a critical review. Bioresource Technology 102 (1), 71–81.

Chisti, Y., 2007. Biodiesel from microalgae. Biotechnology Advances 25 (3), 294–306.

Cohen, Z., 1999. Chemicals from Microalgae. Taylor & Francis, London, UK.

Davies-Colley, R.J., Pridmore, R.D., Hewitt, J.E., 1986. Optical properties of some freshwater phytoplanktonic algae. Hydrobiologia 133 (2), 165–178.

Dubinsky, Z., Stambler, N., 2000. Photoacclimation processes in phytoplankton: mechanisms, consequences, and applications. Aquatic Microbial Ecology 56, 163–176.

Fisher, T., Minnaard, J., Dubinsky, Z., 1996. Photoacclimation in the marine alga *Nannochloropsis* sp. (eustigmatophyte): a kinetic study. Journal of Plankton Research 18 (10), 1797–1818.

Gentile, M.P., Blanch, H.W., 2001. Physiology and xanthophyll cycle activity of *Nannochloropsis gaditana*. Biotechnology and Bioengineering 75 (1), 1–12.

Gitelson, A.A., Grits, Y.A., Etzion, D., Ning, Z., Richmond, A., 2000. Optical properties of *Nannochloropsis* sp. and their application to remote estimation of cell mass. Biotechnology and Bioengineering 69 (5), 516–525.

Hodgson, P., Henderson, R., Sargent, J., Leftley, J., 1991. Patterns of variation in the lipid class and fatty acid composition of *Nannochloropsis oculata*

(eustigmatophyceae) during batch culture. Journal of Applied Phycology 3, 169–181.
Intergovernmental Panel on Climate Change, Climate Change 2007: Impacts, Adaptation and Vulnerability. Contribution of Working Group II to the Fourth Assessment Report of the Intergovernmental Panel on Climate Change. Cambridge University Press, Cambridge, UK, 2007.
Jonasz, M., Fournier, G., 2007. Light Scattering by Particles in Water: Theoretical and Experimental Foundations. Academic Press, San Diego, CA.
Ke, B., 2001. Photosynthesis: Photobiochemistry and Photobiophysics Advances in Photosynthesis. Kluwer Academic Publishers, Dordrecht, The Netherlands.
Lee, E., Heng, R.L., Pilon, L., 2013. Spectral optical properties of selected photosynthetic microalgae producing biofuels. Journal of Quantitative Spectroscopy and Radiative Transfer 114, 122–135.
Lubián, L., Montero, O., Moreno-Garrido, I., Huertas, I., Sobrino, C., González-del Valle, M., Parés, G., 2000. Nannochloropsis (eustigmatophyceae) as source of commercially valuable pigments. Journal of Applied Phycology 12, 249–255.
Ma, X., Lu, J., Brock, R., Jacobs, K., Yang, P., Hu, X., 2003. Determination of complex refractive index of polystyrene microspheres from 370 to 1610 nm. Physics in Medicine and Biology 48 (24), 4165–4172.
Modest, M., 2003. Radiative Heat Transfer. Academic Press, San Diego, CA.
Parsons, T., Stephens, K., Strickland, J., 1961. On the chemical composition of eleven species of marine phytoplanktons. Journal of Fisheries Research Board of Canada 18, 1001–1016.
Pilon, L., 2013. Radiation characteristics of microalgae for CO_2 fixation and biofuel production. Available from: <http://www.seas.ucla.edu/~pilon/downloads.htm>.
Pilon, L., Berberoğlu, H., Kandilian, R., 2011. Radiation transfer in photobiological carbon dioxide fixation and fuel production by microalgae. Journal of Quantitative Spectroscopy and Radiative Transfer 112 (17), 2639–2660.
Pottier, L., Pruvost, J., Deremetz, J., Cornet, J., Legrand, J., Dussap, C., 2005. A fully predictive model for one-dimensional light attenuation by *Chlamydomonas reinhardtii* in a torus photobioreactor. Biotechnology and Bioengineering 91 (5), 569–582.
Rodolfi, L., Zittelli, G.C., Bassi, N., Padovani, G., Biondi, N., Bonini, G., Tredici, M.R., 2009. Microalgae for oil: strain selection, induction of lipid synthesis and outdoor mass cultivation in a low-cost photobioreactor. Biotechnology and Bioengineering 102 (1), 100–112.
Simionato, D., Sforza, E., Carpinelli, E.C., Bertucco, A., Giacometti, G.M., Morosinotto, T., 2011. Acclimation of *Nannochloropsis gaditana* to different illumination regimes: effects on lipids accumulation. Bioresource Technology 102 (10), 6026–6032.
Strickland, J., Parsons, T., 1968. A practical handbook of seawater analysis: pigment analysis. Bulletin of Fisheries Research Board of Canada. Fisheries Research Board of Canada.
Van Vooren, G.V., Grand, F.L., Legrand, J., Cuine, S., Peltier, G., Pruvost, J., 2012. Investigation of fatty acids accumulation in *Nannochloropsis oculata* for biodiesel application. Bioresource Technology 124, 421–432.
Wellburn, A., 1994. The spectral determination of chlorophyll *a* and chlorophyll *b* as well as total carotenoids using various solvents with spectrophotometers of different resolution. Journal of Plant Physiology 144 (3), 307–313.
Zhernovaya, O., Sydoruk, O., Tuchin, V., Douplik, A., 2011. The refractive index of human hemoglobin in the visible range. Physics in Medicine and Biology 56 (13), 4013–4021.
Zou, N., Richmond, A., 2000. Light-path length and population density in photoacclimation of *Nannochloropsis* sp. (eustigmatophyceae). Journal of Applied Phycology 12, 349–354.